Journal of
Innate Immunity

J Innate Immun , DOI: 10.1159/000530249
Received: November 8, 2022
Accepted: March 15, 2023
Published online: April 11, 2023

TLR7 activation in M-CSF-dependent monocyte-derived human macrophages potentiates inflammatory responses and prompts neutrophil recruitment

Simón-Fuentes M, Herrero C, Acero-Riaguas L, Nieto C, Lasala F, Labiod N, Luczkowiak J, Alonso B, Delgado R, Colmenares M, Corbí AL, Domínguez-Soto A

ISSN: 1662-811X (Print), eISSN: 1662-8128 (Online)
https://www.karger.com/JIN
Journal of Innate Immunity

TLR7 activation in M-CSF-dependent monocyte-derived human macrophages potentiates inflammatory responses and prompts neutrophil recruitment

Miriam Simón-Fuentes[1], Cristina Herrero[1], Lucía Acero-Riaguas[1], Concha Nieto[1], Fátima Lasala[2], Nuria Labiod[2], Joanna Luczkowiak[2], Bárbara Alonso[1], Rafael Delgado[2], María Colmenares[1], Ángel L. Corbí[1,3], Ángeles Domínguez-Soto[1,3]

[1] Myeloid Cell Laboratory, Centro de Investigaciones Biológicas, CSIC, Madrid, Spain.
[2] Instituto de Investigación Hospital Universitario 12 de Octubre (imas12), Universidad Complutense School of Medicine, Madrid, Spain.
Short Title: TLR7 functions in human macrophages

[3] ALC and ADS contributed equally to this work.

Corresponding Author: Angeles Domínguez Soto (ads@cib.csic.es), Centro de Investigaciones Biológicas, CSIC. Ramiro de Maeztu, 9. Madrid 28040; Phone: 34-91-8373112.

Number of Tables: 0.
Number of Figures: 5.
Word count: 4170.
Keywords: Macrophages; Inflammatory responses; TLR7; Neutrophil-attracting chemokines

ABSTRACT

Toll-like receptor 7 (TLR7) is an endosomal Pathogen-Associated Molecular Pattern (PAMP) receptor that senses single-stranded RNA (ssRNA) and whose engagement results in the production of type I IFN and pro-inflammatory cytokines upon viral exposure. Recent genetic studies have established that a dysfunctional TLR7-initiated signaling is directly linked to the development of inflammatory responses. We present evidences that TLR7 is preferentially expressed by monocyte-derived macrophages generated in the presence of M-CSF (M-MØ). We now show that TLR7 activation in M-MØ triggers a weak MAPK, NF□B and STAT1 activation and results in low production of type I IFN. Of note, TLR7 engagement re-programs MAFB+ M-MØ towards a pro-inflammatory transcriptional profile characterized by the expression of neutrophil-attracting chemokines (CXCL1-3, CXCL5, CXCL8), whose expression is dependent on the transcription factors MAFB and AhR. Moreover, TLR7-activated M-MØ display enhanced pro-inflammatory responses and a stronger production of neutrophil-attracting chemokines upon secondary stimulation. As aberrant TLR7 signaling and enhanced pulmonary neutrophil/lymphocyte ratio associate with impaired resolution of virus-induced inflammatory responses, these results suggest that targeting macrophage TLR7 might be a therapeutic strategy for viral infections where monocyte-derived macrophages exhibit a pathogenic role.

INTRODUCTION

Macrophages are functionally heterogeneous by virtue of their ontogeny, tissue-specific differentiation and adaptation to the prevailing cytokines, hormones and growth factors in the surrounding extracellular milieu [1–4]. Macrophage Colony-Stimulating Factor (M-CSF), which is indispensable for the generation of most tissue-resident macrophages [5,6], prompts the differentiation of monocyte-derived macrophages (M-MØ) with a MAFB-dependent functional and gene expression profile [7–12]. Remarkably, $MAFB^+$ M-MØ exhibit a huge transcriptional similarity to the subsets of pro-fibrotic and pathogenic pulmonary macrophages identified in severe COVID-19 [13–18]. In fact, M-CSF plasma levels correlate with respiratory failure in COVID-19 [19], and the expression of several biomarkers associated to COVID-19 severity (e.g., CCL2, CCL4, CXCL10)[20–22] is regulated by MAFB [11]. Moreover, SARS-CoV-2 has been recently shown to trigger a MAFB-dependent pro-fibrotic transcriptional response in monocytes [14]. Therefore, the identification of the mechanisms that sustain the effector functions of $MAFB^+$ M-MØ should provide relevant information about the key pathogenic action of macrophages in COVID-19 [23–27].

Unlike GM-CSF-dependent monocyte-derived macrophages (GM-MØ), the transcriptome of $MAFB^+$ M-MØ is characterized by the expression of a gene set ("Anti-inflammatory gene set") which includes the gene encoding Toll-like receptor 7 (*TLR7*) [9,12,28]. TLR7 is an endosomal Pathogen-Associated Molecular Pattern (PAMP) receptor responsible for sensing purine-rich single-stranded ribonucleic acid (ssRNA) from viruses and bacteria by human macrophages [29,30]. TLR7 has been shown to bind ssRNA fragments from SARS-CoV-2 [31–34], and genetic analysis revealed that a dysfunctional TLR7 signaling is responsible for the pathogenesis in a percentage of severe COVID-19 cases [35–42]. Indeed, the continuous activation of TLR7 induces “inflammatory hemophagocytes” that cause macrophage activation syndrome (MAS) and a “cytokine storm” [31,43], features that have been consistently reported in severe COVID-19 patients [23–27]. Typically, TLR7 engagement triggers the production of type I interferon (IFN) and proinflammatory cytokines in human myeloid cells [34,44,45]. However, TLR7 ligands also promote tolerance towards a subsequent stimulation of other TLRs [46–48] and even limit pro-inflammatory activation of human macrophages in atherosclerosis [49]. Besides, and in agreement with its overexpression in M-MØ, TLR7 expression in macrophages is associated to an anti-inflammatory gene profile in cardiovascular diseases [50].

Given the similarities between pathogenic macrophage subsets in COVID-19 and TLR7-expressing MAFB+ M-MØ, we sought to determine the functional and transcriptional consequences of TLR7 engagement in human M-MØ. Surprisingly, TLR7 activation in M-CSF-dependent MAFB+ macrophages failed to trigger an IFN response but elicited the production of neutrophil-attracting chemokines and pushed macrophages towards the acquisition of a stronger pro-inflammatory phenotype and gene profile. These results pose TLR7 as a potential target for the design of macrophage-reprogramming therapeutic strategies in viral infections where monocyte-derived macrophages have a prominent pathogenic role.

MATERIALS AND METHODS

Generation of human monocyte-derived macrophages *in vitro* and treatments. Human Peripheral Blood Mononuclear Cells (PBMCs) were isolated from buffy coats from anonymous healthy donors over a Lymphoprep (Nycomed Pharma) gradient according to standard procedures. Monocytes were purified from PBMC by magnetic cell sorting using anti-CD14 microbeads (Miltenyi Biotec). Monocytes (>95% $CD14^+$ cells) were cultured at 0.5 x 10^6 cells/ml in RPMI 1640 (Gibco) medium supplemented with 10% fetal bovine serum (FBS) for 7 days in the presence of 1000 U/ml GM-CSF or 10 ng/ml M-CSF (ImmunoTools) to generate GM-CSF-polarized macrophages (GM-MØ) or M-CSF-polarized macrophages (M-MØ), respectively [11]. Cytokines were added every two days and cells were maintained at 37°C in a humidified atmosphere with 5% CO_2 and 21% O_2. For macrophage activation, cells were treated with 1 □g/ml CL264 (Invivogen), unless otherwise indicated, or 10 ng/ml E. coli 055:B5 lipopolysaccharide (Ultrapure LPS, Sigma-Aldrich) [51]. Where indicated, Enpatoran (MCE MedChem Express) or TLR7/8-IN-1 (MCE MedChem Express) were added 1 hour before exposure to CL264. Human cytokine and chemokine production were measured in M-MØ culture supernatants using commercial ELISA for CCL2, CXCL1, CXCL5, CXCL8, CXCL10, TNF, IL-6, IL-10, IL-12p40 or IFN□1 following the procedures supplied by the manufacturers.

Quantitative real-time RT-PCR (qRT-PCR). Total RNA was extracted using the total RNA and protein isolation kit (Macherey-Nagel). RNA samples were reverse-transcribed with High-Capacity cDNA Reverse Transcription reagents kit (Applied Biosystems) according to the manufacturer's protocol. Real-time quantitative PCR was performed with LightCycler® 480 Probes Master (Roche Life Sciences) and Taqman probes on a standard plate in a Light Cycler® 480 instrument (Roche Diagnostics). Gene-specific oligonucleotides were designed using the Universal ProbeLibrary software (Roche Life Sciences). Results were normalized to the expression level of the endogenous references genes *TBP* and *HPRT1*, and quantified using the ΔΔCT (cycle threshold) method.

Western blot. Western blot was carried out following previously described procedures [11] and using antibodies against TLR7 (#5632, Cell Signaling), MAFB (HPA005653, Sigma Aldrich), MAF (sc-7866; Santa Cruz Biotechnology), AhR (sc-133088, Santa Cruz Biotechnology), phosphorylated and total ERK1/2, p38MAPK and JNK (Cell Signaling), phosphorylated STAT1 and STAT3 (BD Biosciences), I□B□, and phosphorylated CREB (Cell Signaling). Protein loading was normalized using a monoclonal antibody against GAPDH (sc-32233, Santa Cruz) or vinculin (V9131, Sigma-Aldrich). Chemiluminiscence was detected in a Chemidoc Imaging system (BioRad) using SuperSignal™ West Femto (ThermoFisher Scientific).

Small Interfering Ribonucleic Acid (siRNA) Transfection. M-MØ (1 × 10^6 cells) were transfected with a human MAFB-specific siRNA (siMAFB, 25 nM, SMARTpool Dharmacon), human MAF-specific siRNA (siMAF, 25 nM, SMARTpool Dharmacon) or human AhR-specific siRNA (siAHR, 50nM, #s1199 Thermo Scientific) using HiPerFect (Qiagen). Silencer™ Select Negative Control No. 1 siRNA (siCNT, 50 nM) (Dharmacon) was used as negative control siRNA. Six hours after transfection, cells were allowed to recover from transfection in complete medium (18 h) and subjected to the indicated treatments. Knock-down of MAFB, MAF and AhR was confirmed by q-PCR and western blot.

RNA-sequencing and data analysis. Total RNA was extracted from preparations of M-MØ derived from three independent donors, and exposed to LPS (10ng/ml), CL264 (1□g/ml) or left untreated for 0.5, 2, 4 or 12 hours, and library preparation, fragmentation and sequencing were performed at BGI (https://www.bgitechsolutions.com) using the BGISEQ-500 platform (Gene Expression Omnibus (GEO) accession no. GSE156921) [12]. Following the same procedure, RNA-seq was performed on three independent preparations of M-MØ exposed to CL264 after siRNA-mediated silencing of either MAFB, MAF or AhR, using the BGISEQ-500 platform, and data were deposited in GEO (http://www.ncbi.nlm.nih.gov/geo/) under accession no. GSE181249 and GSE205719. Differentially expressed genes were analyzed for annotated gene sets enrichment using Enrichr (http://amp.pharm.mssm.edu/Enrichr/) [52,53], and enrichment terms considered significant with a Benjamini-Hochberg-adjusted p value <0.05. For gene set enrichment analysis (GSEA) (http://software.broadinstitute.org/gsea/index.jsp) [54], gene sets available at the website, as well as gene sets generated from publicly available transcriptional studies (https://www.ncbi.nlm.nih.gov/gds), were used. The gene sets that define the transcriptome of human monocyte-derived pro-inflammatory GM-MØ-specific "Pro-inflammatory gene set" and the M-MØ-specific "Anti-inflammatory gene set" have been previously reported

(GSE68061) [9][28]. Gene expression in breast carcinoma was assessed using the METABRIC (Molecular Taxonomy of Breast Cancer International Consortium) study cohort [55,56] on the CBioportal (http://www.cbioportal.org).

Neutrophil isolation and transmigration assays. Neutrophils were obtained from peripheral blood from anonymous healthy donors over a Polymorphprep (Progen) gradient according to manufacturer procedures. Neutrophil purity was assessed by flow cytometry (>95% CD15+ cells) (CD15 Monoclonal Antibody, APC, Invitrogen Cat. Nº 17-0158-41). Neutrophil migration assays were performed following the protocol previously described [57] with some modifications. Briefly, $2x10^5$ neutrophils were added on top of the Transwell inserts (6.5 mm Transwell® with 3.0 µm Pore Polycarbonate Membrane Insert, Corning 3415) in 200 µl of complete EGM-2MV medium (Lonza, CC-3202). The lower compartment was then filled with 600 µl of conditioned medium from untreated or CL264-treated M-MØ, RPMI-10% FBS as negative control, or 50 ng/ml recombinant human IL-8 (Immunotools) in RPMI-10% FBS as positive control. Migration was allowed for 1 h and migrated neutrophils were quantified by Flow Cytometry (Cytfolex-S, Beckman-Coulter).

Statistical analysis. For comparison of means, and unless otherwise indicated, statistical significance of the generated data was evaluated using the paired Student t test or ratio paired
t test. In all cases, $p<0.05$ was considered as statistically significant.

RESULTS

TLR7 expression marks macrophages with an anti-inflammatory profile. We have previously determined the transcriptome of M-CSF-dependent (M-MØ) and GM-CSF-dependent (GM-MØ) monocyte-derived macrophages (GSE68061) and found that *TLR7* belongs to the M-MØ-specific "Anti-inflammatory gene set" [9,28] (Fig. 1A). In fact, TLR7 protein (both the full-length 140 kDa form and the proteolytically processed mature 75 kDa form) was found to be expressed at much higher levels in M-MØ than in GM-MØ (Fig. 1B). Further analysis revealed that *TLR7* is specifically upregulated along the monocyte-to-M-MØ differentiation (GSE188278) (Fig. 1C) and that GM-CSF has a negative effect on *TLR7* expression (Fig. 1D). These results indicate that *TLR7* expression marks macrophages with anti-inflammatory potential, a suggestion reinforced by the higher *TLR7* expression observed in M-MØ from a Multicentric Carpo-Tarsal Osteolysis patient (Fig. 1E), a disease caused by *MAFB* mutations which enhance MAFB protein stability and whose macrophages exhibit a stronger anti-inflammatory gene profile [11] (GSE155883). Further supporting its preferential expression in anti-inflammatory macrophages [50], *TLR7* was also higher in IL-10-producing LPS-activated M-MØ [12] (Fig. 1F), and was detected in *MAFB*$^{+}$ *FOLR2+* macrophages in the fetal-maternal interface [58] (Fig. 1G). Besides, *TLR7* expression significantly correlated with that of numerous M-CSF-dependent genes in breast cancer (METABRIC Cohort, Supplementary Figure 1A, 1B), including the tumor-associated macrophage marker FOLR2 [59,60], and was elevated in human breast cancer tumor-associated macrophages [61] (GSE117970, Supplementary Figure 1C). Hence, *TLR7* is preferentially expressed in macrophages with an anti-inflammatory and immunosuppressive transcriptional profile.

TLR7 activation results in the acquisition of a unique transcriptional and cytokine profile. Since M-MØ exposure to TLR2 or TLR4 ligands leads to the preferential production of IL-10 [12], we next assessed the response of M-MØ to TLR7 activation by using the TLR7-specific ligand CL264. Exposure to CL264 induced the release of IL-10, TNF, IL-6, and IL-12p40, and enhanced CCL2 production (Supplementary Figure 2A), thus demonstrating the functionality of TLR7 in M-MØ. Regarding TLR7-initiated intracellular signaling in M-MØ (Fig. 2A), and compared to the paradigmatic macrophage-activating agent LPS, TLR7 activation led to weaker activation of ERK, and p38MAPK, an almost absent JNK phosphorylation, a more transient activation of NF□B (Fig. 2B) and lower STAT1 phosphorylation at longer time points (Fig. 2C, Supplementary Figure 2B). By contrast, no significant difference was found between CL264- and LPS-induced phosphorylation of STAT3 and CREB (Fig. 2C, Supplementary Figure 2B). In agreement with their distinct intracellular signaling, LPS and CL264 also differentially modulated the production of pro-inflammatory cytokines and IL-10, with TLR7 activation resulting in higher release of IL-12p40 and IL-6, but lower production of IL-10 and the IFN-inducible CXCL10 chemokine (Fig. 2D, E). Remarkably, and unlike LPS, TLR7 activation did not stimulate the production of IFN□1 (Fig. 2E), a result that fits with the weak STAT1 phosphorylation promoted by CL264 (Fig. 2C). Thus, TLR7 activation of M-MØ promotes the acquisition of a unique cytokine profile in which the lack of IFN□1 and weak production of CXCL10 are especially noteworthy.

To examine the extent of the specificity of TLR7-initiated gene changes, the transcriptome of M-MØ exposed to either a TLR7-specific ligand (CL264) or LPS was compared at different time points (GSE156921, Fig. 2F). Exposure to CL264 caused a profound transcriptional change in M-MØ at all-time points (Supplementary Figure 2C), and large differences were observed among the transcriptomes of LPS- and CL264-treated M-MØ (Supplementary Figure 2D). Of note, and unlike LPS-treated M-MØ, M-MØ showed no expression of *IFNB1* after exposure to CL264 for 0.5h, 2h and 4h (Fig. 2G). Further stressing the lack of IFN□1 production after TLR7 activation in M-MØ, gene ontology analysis showed a huge difference in the expression of the "Interferon alpha/beta signaling Homo sapiens R-HSA-909733" gene set (Reactome_2016 gene set library) (https://reactome.org) in LPS-treated M-MØ and CL264-treated M-MØ at all time points (Fig. 2H), and the enrichment of interferon-related gene sets in the genes with higher (>4 times) expression in LPS-treated M-MØ after 2 and 4 hr, (https://maayanlab.cloud/Enrichr/) (Supplementary Figure 2E). Therefore, TLR7 activation of M-MØ promotes transcriptional changes characterized by the remarkable lack of expression of IFN□1 and a very weak expression of type I IFN-inducible genes.

TLR7 activation in M-MØ induces a pro-inflammatory transcriptional signature and potentiates the production of pro-inflammatory cytokines upon exposure to a secondary stimulus. Previous studies have shown that TLR7 activation drives the generation of inflammatory hemophagocytes resembling splenic red pulp macrophages [43] and

can also re-program M-CSF-treated monocytes towards an anti-fibrotic phenotype [62]. As a means to evaluate whether TLR7 activation modifies the polarization state of M-MØ, we measured the expression of paradigmatic polarization-specific markers after a 24h exposure to CL264 (Fig. 3A). TLR7 activation caused a very significant decrease in the expression of genes that best define the transcriptome of anti-inflammatory M-MØ (Fig. 3B, C). Conversely, CL264-treated M-MØ exhibited a higher expression of genes that mark the pro-inflammatory profile of GM-CSF-dependent monocyte-derived macrophages (GM-MØ) (Fig. 3B, C). Therefore, TLR7 activation results in the acquisition of the transcriptome that characterizes pro-inflammatory GM-MØ. Since M-MØ and GM-MØ greatly differ in their activation-induced cytokine production [9,28], we next hypothesized that TLR7-activated M-MØ might also display an altered cytokine profile upon subsequent activation. To address this hypothesis, M-MØ were exposed to CL264 for 24 hours and, after extensive washing, CL264-treated M-MØ were subjected to a secondary stimulation with either CL264 or LPS (Fig. 3D). The modulatory action of TLR7 on M-MØ responses was evident at the intracellular signaling level, because CL264-treated M-MØ exhibited a weaker LPS-induced activation of ERK, JNK and NF□B, and a complete loss of LPS- and CL264-induced STAT3 activation (Fig. 3E, Supplementary Figure 2F). In line with these findings, and compared to unstimulated cells, CL264-treated M-MØ showed a much higher production of IL-6, TNF and CXCL10 after activation with LPS as a secondary stimulus (Fig. 3F). By contrast, exposure to CL264 led to a diminished release of IL-10 in response to LPS (Fig. 3F). Therefore, activation of CL264-treated M-MØ by a secondary stimulus results in enhanced production of pro-inflammatory cytokines and reduced levels of IL-10. These results, which are compatible with the loss of the characteristic gene profile of CL264-treated M-MØ, indicate that TLR7 activation conditions macrophages for stronger pro-inflammatory responses upon encounter with subsequent stimuli, an effect that evokes "trained immunity" events initiated from other PAMP receptors.

TLR7 activation in M-CSF-dependent M-MØ induces the expression of neutrophil-attracting chemokines. To further examine the response of M-MØ to TLR7 activation, we focused on those genes whose expression in LPS-treated M-MØ and CL264-treated M-MØ differed by at least 8-fold (|log2FC|>3) at any time point (GSE156921) (Fig. 4A). k-means clustering of these 467 genes allowed the identification of a group of genes (Cluster 2, 33 genes) exclusively upregulated in CL264-treated M-MØ at late time points (Fig. 4A, Supplementary Figure 3A), and whose expression was clearly distinct from those only upregulated in LPS-treated M-MØ, which included IFN-dependent genes (Clusters 1, 3 and 4) (Fig. 4A, Supplementary Figure 3A,B). Cluster 2 grouped numerous chemokine-encoding genes (*CXCL1*, *CXCL3*, *CXCL5*, *CXCL6, PPBP/CXCL7* and *CXCL8*) (Fig. 4A), whose expression reached maximal values in CL264-treated M-MØ after 12h (Fig. 4B). By contrast, the expression of IFN-regulated chemokine-encoding genes (*CXCL9*, *CXL10*, *CXCL11*) was maximal at later time points only in LPS-treated M-MØ (Fig. 4B, Supplementary Figure 3A, B). As the chemokines encoded by the genes in Cluster 2 belong to the ELR+ CXC granulocyte-attracting chemokine subfamily [63], the importance of their elevated expression is supported by the robust enrichment of the GO Biological Process terms "GOBP_NEUTROPHIL_CHEMOTAXIS" and "GOBP_ NEUTROPHIL _MIGRATION" in CL264-treated M-MØ after 12h of stimulation (Fig. 4C, Supplementary Figure 3C). Indeed, CL264-treated M-MØ released high levels of CXCL1, CXCL5 and CXCL8, while LPS-treated M-MØ released higher levels of CXCL10 (Fig. 4D). In fact, conditioned medium from CL264-treated M-MØ showed a greatly elevated ability for neutrophil recruitment in transmigration experiments (Fig. 4E), whereas the monocyte-recruiting ability of M-MØ and CL264-treated M-MØ did not differ significantly (Supplementary Figure 3D). Consequently, TLR7 activation of M-MØ does not lead to IFN□1 production but results in the induction of numerous ELR+ CXC chemokines with neutrophil-attracting ability. Of note, pre-treatment of M-MØ with TLR7 inhibitors Enpatoran [64] or TLR7/8-IN-1 (https://patentscope.wipo.int/search/en/detail.jsf?docId=WO2019220390) dose-dependently abrogated the CL264-induced production of CXCL1, CXCL5 and CXCL8 (Supplementary Figure 3E), thus demonstrating that the production of CXCL chemokines by CL264-activated M-MØ is TLR7-dependent. Besides, and like in the case of pro-inflammatory cytokines, CL264-treated M-MØ also exhibited an augmented production of neutrophil-attracting chemokines (CXCL1, CXCL5, CXCL8) when exposed to additional pathogenic stimuli (Fig. 4F), further illustrating the functional significance of TLR7 ligation in M-MØ.

Acquisition of the TLR7-induced neutrophil-recruiting chemokine production is dependent on the macrophage polarization state. As *TLR7* is preferentially expressed in macrophages (M-MØ) whose gene profile is dependent on MAFB [11,65], MAF [18,66] and AhR [67,68], we next assessed whether macrophage re-programming prevented the

acquisition of the TLR7-initiated transcriptome and the production of CXCL chemokines. To that end, MAFB, MAF or AhR were knocked-down in M-MØ before TLR7 activation (Fig. 5A, Supplementary Figure 4A), and transcriptional analysis performed on the resulting cells (GSE181249, GSE205719). Compared to M-MØ transfected with a control siRNA (siCNT M-MØ), knockdown of AhR (siAHR M-MØ) completely abrogated the upregulation of the "GOBP_NEUTROPHIL_CHEMOTAXIS" gene set, whose expression was also impaired after MAFB knockdown - (Supplementary Figure 4B). Along the same line, GSEA confirmed that knockdown of either AhR or MAFB, but not MAF, very significantly reduced the expression of the CL264-specific Cluster 2 genes (Fig. 5B, Supplementary Figure 4C). Specifically, AhR knockdown impaired the CL264-mediated upregulation of *CXCL1*, *CXCL2*, *CXCL3*, *CXCL5* and *CXCL8* gene expression, while MAFB knockdown limited the expression of the *CXCL1* gene (Fig. 5C). Indeed, determination of chemokine production in CL264-treated siAHR M-MØ, siMAFB M-MØ and siMAF M-MØ (Fig. 5D) revealed that knock-down of either AhR or MAFB significantly reduces the production of the neutrophil-recruiting chemokines CXCL1, CXCL5 and CXCL8 (Fig. 5E). Therefore, these results demonstrate that the macrophage polarization state determines the extent of the response to TLR7 activation, and indicate that the AhR- and MAFB-dependent anti-inflammatory state of M-MØ is required for TLR7 activation to trigger the production of neutrophil-recruiting chemokines.

DISCUSSION

Several reports have now identified the monocyte-derived pulmonary macrophage subsets that are responsible for severe COVID-19 [13–16] and whose transcriptional signature resembles that of M-CSF-dependent monocyte-derived macrophages (M-MØ) [14,18]. As TLR7 is significantly over-expressed in M-MØ [9,12,28], and its defective signaling is linked to COVID-19 severity [35–42], we have now assessed the transcriptional and functional outcome of TLR7 activation in M-MØ. Our results indicate that TLR7 ligation in M-MØ results in absent type I IFN production but in strong production of neutrophil-recruiting "CXCL" chemokines, all of which would promote pathologic parameters described in severe COVID-19 like impaired viral elimination and enhanced accumulation of neutrophils in infected tissues. Besides, we have found that the TLR7-initiated "CXCL" chemokine production is dependent on the transcription factors MAFB and AhR, which are major determinants of the anti-inflammatory profile of human macrophages.

The pattern of expression of TLR7 in human macrophages under physiological and pathological conditions also lends relevance to our findings on the TLR7 function in M-CSF-dependent monocyte-derived macrophages (Fig. 1), as TLR7 is expressed by the M2 macrophage subset in calcific aortic valve stenosis [50], and by decidual macrophages [58] (Supplementary Figure 1A) and Tumor-Associated Macrophages (Supplementary Figure 1B), both of which display immunosuppressive functions. Like in M-MØ , TLR7 expression is detected in FOLR2-expressing macrophages in the fetal-maternal interface [58] and in FOLR2+ TAM [59,60], and the co-expression of FOLR2 and TLR7 in TAM and monocyte-derived macrophages has been used for macrophage functional re-programming *in vitro* and *in vivo* [60,62]. Specifically, a folate-targeted TLR7 agonist has been already used to reduce the immunosuppressive, pro-tumoral and pro-metastatic function of TAM [60] and, more recently, to re-program fibrosis-inducing into fibrosis-suppressing macrophages in a bleomycin-induced pulmonary fibrosis mouse model [62]. Considering the pro-fibrotic phenotype of the pathogenic pulmonary macrophages in severe SARS-CoV-2 infections [14], these antecedents support the therapeutic potential of TLR7 agonists in COVID-19. Our results complement and extend these previous studies by providing the molecular basis for the TLR7-initiated intracellular signaling and gene signature in human monocyte-derived macrophages, and raise the possibility that the TLR7-driven macrophage re-programming action *in vivo* might derive from the ability of TLR7 to potentiate the production of pro-inflammatory cytokines upon exposure to secondary stimuli.

As the ligation of TLR7 triggers the release of type I IFN in other cell types [69–71], the lack of production of type I IFN by TLR7-activated M-MØ that we have observed is unexpected and indicates that M-MØ exhibit a defective TLR7-type I IFN link. In this regard, although LPS-activated M-MØ produce much lower levels of IFN□1 than LPS-stimulated GM-CSF-dependent macrophages [12], the expression of *IFNB1* in TLR7-activated M-MØ is even lower than in LPS-activated M-MØ and, in fact, no IFN□1 protein expression can be detected in the supernatant of TLR7-activated M-MØ. The absence of IFN□1 expression by TLR7-activated M-MØ might derive from the strong IL-10-dependent STAT3 activation observed in activated M-MØ [12] and the ability of STAT3 to inhibit the STAT1-mediated IFN type I response [72–74]. Conversely, the strong release of neutrophil-attracting chemokines at late time points (12 hours) after TLR7 activation is unexpected, because it does not occur upon TLR4 stimulation. The late production of “CXCL" chemokines in TLR7-activated M-MØ, but not in LPS-activated M-MØ, might be related to the distinct kinetics of *IL10* expression in both cases, as *IL10* levels are considerably reduced at late time points only in TLR7-activated M-MØ, but sustained in LPS-activated M-MØ [12]. The link between low *IL10* expression and high expression of *CXCL8* also agrees with the higher expression of other IL-10-regulated genes at late time points after TLR7 ligation, including *IL1A* and *IL6*. Noteworthy, If the kinetics of *IL10* is similar after TLR7 stimulation in pro-fibrotic pulmonary monocyte-derived macrophages, it would lead to: 1) excessive/deregulated levels of pro-inflammatory cytokines, including IL-6, a feature that also characterizes severe COVID-19; and 2) increased neutrophil recruitment towards lungs after SARS-CoV-2 infection [75,76]. Thus, the "TLR7-CXCL" axis might be of particular relevance, because myeloid cell-derived neutrophil chemotaxis is related to severity of COVID-19 [76–78], for which even CXCR2 antagonists have been proposed as a treatment [79].

An additional finding with pathological implications is the ability of TLR7 to condition the response of M-MØ to subsequent stimuli. Previous reports have described that TLR activation leads to tolerance towards other TLR ligands

[46–48] and also limits the pro-inflammatory activation of macrophages [49]. By contrast, whereas the tolerance against further TLR7 stimulation was also seen in M-MØ, our results indicated that TLR7-activated M-MØ exhibit a strong shift in their gene expression profile and respond to secondary stimuli by producing much higher levels of proinflammatory cytokines, including TNF and IL-6. Although observed upon a short (24h) exposure to the TLR7 ligand, this conditioning action of TLR7 activation resembles the macrophage "training" ability of other pathogen-derived products, like the TLR2 ligand □-glucan [80]. As viral respiratory infections predispose to bacterial infections, and bacterial co-infections have a worse outcome than either infection [81], the macrophage "training" ability of TLR7 might be of importance in the case of COVID-19, where concomitant infection by other pathogens (viruses, bacteria including mycobacteria, fungi) might be implicated in the excessive pro-inflammatory response that takes place in lungs of severe patients [81], and whose presence would constitute a secondary stimulation for macrophages previously activated by SARS-CoV-2. Along the same line, it is worth noting that diabetes and obesity, two of the most relevant risk factors for severe COVID-19 [82], are associated with elevated levels of palmitate [83–85], itself a promoter of pro-inflammatory activation of human macrophages [51]. Thus, it is tempting to speculate that palmitate exposure of "TLR7-trained" macrophages might exacerbate the strong pro-inflammatory response that occurs in obese or diabetes patients in response to SARS-CoV-2 infection.

ACKNOWLEDGMENT. We thank Dr. Miguel A. Vega for valuable suggestions and critically reading the manuscript.

STATEMENT OF ETHICS. Research was conducted ethically in accordance with the World Medical Association Declaration of Helsinki. This study protocol was reviewed and approved by Comisión de Investigación del Centro de Transfusión (approval number 28504/02) and written informed consents were obtained from donors by Centro de Transfusión (26/7/2021).

CONFLICT OF INTEREST STATEMENT. The authors have no conflicts of interest to declare.

FUNDING SOURCES. This work was supported by Grant PID2020-114323RB-I00 from Ministerio de Ciencia e Innovación, "Ayudas FUNDACIÓN BBVA a equipos de investigación científica SARS-CoV-2 y COVID-19" and Grant 201619.31 from Fundació La Marató/TV3 to ALC, grants from the Instituto de Investigación Carlos III, ISCIII, (PI2100989), European Commission Horizon 2020 FP (Project VIRUSCAN FETPROACT-2016: ID 731868), Horizon Europe FP (Project EPIC-CROWN-2 ID: 101046084) and Fundación Caixa-Health Research (Project StopEbola HR18-00469) to RD, and Red de Investigación en Enfermedades Reumáticas (RIER, RD16/0012/0007), and co-financed by the European Regional Development Fund "A way to achieve Europe" (ERDF) to ALC. This research work was also funded by the European Commission – NextGenerationEU (Regulation EU 2020/2094), through CSIC's Global Health Platform (PTI Salud Global). MSF was funded by a Formación de Personal Investigador predoctoral fellowship from Ministerio de Ciencia e Innovación (Grant PRE2018-083396).

AUTHOR CONTRIBUTIONS. Miriam Simón-Fuentes, Cristina Herrero, Lucía Acero-Riaguas, Concha Nieto, Fátima Lasala, Nuria Labiod, Joanna Luczkowiak, Bárbara Alonso, María Colmenares and Ángeles Domínguez-Soto performed research and analyzed data; María Colmenares, Rafael Delgado, Ángel L. Corbí, and Ángeles Domínguez-Soto designed the research and analyzed data; Ángel L. Corbí, and Ángeles Domínguez-Soto wrote the paper.

DATA AVAILABILITY STATEMENT. The data that support the findings of this study are available in Gene Expression Omnibus (GEO) at http://www.ncbi.nlm.nih.gov/geo/ under accession no. GSE156921, GSE181249 and GSE205719. Further enquiries can be directed to the corresponding author.

REFERENCES

1 Locati M, Curtale G, Mantovani A. Diversity, Mechanisms, and Significance of Macrophage Plasticity. Annu Rev Pathol Mech Dis. 2020 Jan;15:123–47.

2 Wynn TA, Vannella KM. Macrophages in Tissue Repair, Regeneration, and Fibrosis. Immunity. 2016 Mar;44(3):450–62.

3 Lavin Y, Mortha A, Rahman A, Merad M. Regulation of macrophage development and function in peripheral tissues. Nat Rev Immunol. 2015;15(12):731–44.

4 Italiani P, Boraschi D. Development and functional differentiation of tissue-resident versus monocyte-derived macrophages in inflammatory reactions. Results Probl Cell Differ. 2017;62:23–43.

5 Yamamoto T, Kaizu C, Kawasaki T, Hasegawa G, Umezu H, Ohashi R, et al. Macrophage colony-stimulating factor is indispensable for repopulation and differentiation of Kupffer cells but not for splenic red pulp macrophages in osteopetrotic (op/op) mice after macrophage depletion. Cell Tissue Res. 2008;332(2):245–56.

6 Hamilton JA. Colony-stimulating factors in inflammation and autoimmunity. Nat Rev Immunol. 2008;8(7):533–44.

7 Fleetwood AJ, Dinh H, Cook AD, Hertzog PJ, Hamilton JA. GM-CSF- and M-CSF-dependent macrophage phenotypes display differential dependence on Type I interferon signaling. J Leukoc Biol. 2009;86(2):411–21.

8 Verreck FAW, De Boer T, Langenberg DML, Hoeve MA, Kramer M, Vaisberg E, et al. Human IL-23-producing type 1 macrophages promote but IL-10-producing type 2 macrophages subvert immunity to (myco)bacteria. Proc Natl Acad Sci U S A. 2004;101(13):4560–5.

9 Sierra-Filardi E, Puig-Kröger A, Blanco FJ, Nieto C, Bragado R, Palomero MI, et al. Activin A skews macrophage polarization by promoting a proinflammatory phenotype and inhibiting the acquisition of anti-inflammatory macrophage markers. Blood. 2011;117(19):5092–101.

10 Pyonteck SM, Akkari L, Schuhmacher AJ, Bowman RL, Sevenich L, Quail DF, et al. CSF-1R inhibition alters macrophage polarization and blocks glioma progression. Nat Med. 2013;19(10):1264–72.

11 Cuevas VD, Anta L, Samaniego R, Orta-Zavalza E, Vladimir de la Rosa J, Baujat G, et al. MAFB Determines Human Macrophage Anti-Inflammatory Polarization: Relevance for the Pathogenic Mechanisms Operating in Multicentric Carpotarsal Osteolysis. J Immunol. 2017;198(5):2070–81.

12 Cuevas VD, Simón-Fuentes M, Orta-Zavalza E, Samaniego R, Sánchez-Mateos P, Escribese M, et al. The gene signature of activated M-CSF-Primed human monocyte-derived macrophages is IL-10-dependent. J Innate Immun. 2022;14(3):243–25.

13 Liao M, Liu Y, Yuan J, Wen Y, Xu G, Zhao J, et al. Single-cell landscape of bronchoalveolar immune cells in patients with COVID-19. Nat Med. 2020;26(6):842–4.

14 Wendisch D, Dietrich O, Mari T, von Stillfried S, Ibarra IL, Mittermaier M, et al. SARS-CoV-2 infection triggers profibrotic macrophage responses and lung fibrosis. Cell. 2021 Dec;184(26):6243-6261.e27.

15 Grant RA, Morales-Nebreda L, Markov NS, Swaminathan S, Querrey M, Guzman ER, et al. Circuits between infected macrophages and T cells in SARS-CoV-2 pneumonia. Nature. 2021 Feb;590(7847):635–41.

16 Zhang F, Mears JR, Shakib L, Beynor JI, Shanaj S, Korsunsky I, et al. IFN-γ and TNF-α drive a CXCL10+ CCL2+ macrophage phenotype expanded in severe COVID-19 lungs and inflammatory diseases with tissue inflammation. Genome Med. 2021 Apr;13(1):64.

17 Joshi N, Watanabe S, Verma R, Jablonski RP, Chen CI, Cheresh P, et al. A spatially restricted fibrotic niche in pulmonary fibrosis is sustained by M-CSF/M-CSFR signalling in monocyte-derived alveolar macrophages. Eur Respir J. 2020 Jan;55(1):1900646.

18 Vega MA, Simón-Fuentes M, González de la Aleja A, Nieto C, Colmenares M, Herrero C, et al. MAFB and MAF Transcription Factors as Macrophage Checkpoints for COVID-19 Severity. Front Immunol. 2020;11:603507.

19 Quartuccio L, Fabris M, Sonaglia A, Peghin M, Domenis R, Cifù A, et al. Interleukin 6, soluble interleukin 2 receptor alpha (CD25), monocyte colony-stimulating factor, and hepatocyte growth factor linked with systemic hyperinflammation, innate immunity hyperactivation, and organ damage in COVID-19 pneumonia. Cytokine. 2021 Apr;140:155438.

20 Yang Y, Shen C, Li J, Yuan J, Wei J, Huang F, et al. Plasma IP-10 and MCP-3 levels are highly associated with disease severity and predict the progression of COVID-19. J Allergy Clin Immunol. 2020 Jul;146(1):119-127.e4.

21 Trump S, Lukassen S, Anker MS, Chua RL, Liebig J, Thürmann L, et al. Hypertension delays viral clearance and exacerbates airway hyperinflammation in patients with COVID-19. Nat Biotechnol. 2021 Jun;39(6):705–16.
22 Chen Y, Wang J, Liu C, Su L, Zhang D, Fan J, et al. IP-10 and MCP-1 as biomarkers associated with disease severity of COVID-19. Mol Med. 2020 Dec;26(1):97.
23 Merad M, Martin JC. Pathological inflammation in patients with COVID-19: a key role for monocytes and macrophages. Nat Rev Immunol. 2020;20(6):355–62.
24 Boumaza A, Gay L, Mezouar S, Bestion E, Diallo AB, Michel M, et al. Monocytes and Macrophages, Targets of Severe Acute Respiratory Syndrome Coronavirus 2: The Clue for Coronavirus Disease 2019 Immunoparalysis. J Infect Dis. 2021 Aug;224(3):395–406.
25 Schulte-Schrepping J, Reusch N, Paclik D, Baßler K, Schlickeiser S, Zhang B, et al. Severe COVID-19 Is Marked by a Dysregulated Myeloid Cell Compartment. Cell. 2020 Sep;182(6):1419-1440.e23.
26 Pence BD. Severe COVID-19 and aging: are monocytes the key? GeroScience. 2020 Aug;42(4):1051–61.
27 Knoll R, Schultze JL, Schulte-Schrepping J. Monocytes and Macrophages in COVID-19. Front Immunol. 2021 Jul;12:2952.
28 González-Domínguez É, Domínguez-Soto Á, Nieto C, Flores-Sevilla JL, Pacheco-Blanco M, Campos-Peña V, et al. Atypical Activin A and IL-10 Production Impairs Human CD16 + Monocyte Differentiation into Anti-Inflammatory Macrophages. J Immunol. 2016;196(3):1327–37.
29 Diebold SS, Kaisho T, Hemmi H, Akira S, Reis E Sousa C. Innate Antiviral Responses by Means of TLR7-Mediated Recognition of Single-Stranded RNA. Science (80-). 2004;303(5663):1529–31.
30 Gantier MP, Tong S, Behlke MA, Xu D, Phipps S, Foster PS, et al. TLR7 is involved in sequence-specific sensing of single-stranded RNAs in human macrophages. J Immunol. 2008 Feb;180(4):2117–24.
31 Manik M, Singh RK. Role of toll-like receptors in modulation of cytokine storm signaling in SARS-CoV-2-induced COVID-19. J Med Virol. 2022;94(3):869–77.
32 Moreno-Eutimio MA, López-Macías C, Pastelin-Palacios R. Bioinformatic analysis and identification of single-stranded RNA sequences recognized by TLR7/8 in the SARS-CoV-2, SARS-CoV, and MERS-CoV genomes. Microbes Infect. 2020;22(4–5):226–9.
33 Bortolotti D, Gentili V, Rizzo S, Schiuma G, Beltrami S, Strazzabosco G, et al. Tlr3 and tlr7 rna sensor activation during sars-cov-2 infection. Microorganisms. 2021;9(9):1820.
34 Salvi V, Nguyen HO, Sozio F, Schioppa T, Laffranchi M, Scapini P, et al. SARS-CoV-2-associated ssRNAs activate inflammation and immunity via TLR7/8. JCI Insight. 2021;6(18):1–15.
35 Englmeier L, Subburayalu J. What's happening where , when SARS-CoV-2 infects : are TLR7 and MAFB sufficient to explain patient vulnerability ? 2022;3:4–11.
36 VAN DE VEERDONK FL, Netea MG. Covid-19 rare variants increase the risk of severe covid-19. Elife. 2021;10:e67860.
37 Abolhassani H, Vosughimotlagh A, Asano T, Landegren N, Boisson B, Delavari S, et al. X-Linked TLR7 Deficiency Underlies Critical COVID-19 Pneumonia in a Male Patient with Ataxia-Telangiectasia. J Clin Immunol. 2022;42(1):1–9.
38 Van Der Made CI, Simons A, Schuurs-Hoeijmakers J, Van Den Heuvel G, Mantere T, Kersten S, et al. Presence of Genetic Variants among Young Men with Severe COVID-19. JAMA - J Am Med Assoc. 2020;324(7):663–73.
39 Solanich X, Vargas-Parra G, van der Made CI, Simons A, Schuurs-Hoeijmakers J, Antolí A, et al. Genetic Screening for TLR7 Variants in Young and Previously Healthy Men With Severe COVID-19. Front Immunol. 2021;12(July):1–10.
40 Fallerini C, Daga S, Mantovani S, Benetti E, Picchiotti N, Francisci D, et al. Association of toll-like receptor 7 variants with life-threatening COVID-19 disease in males: Findings from a nested case-control study. Elife. 2021;10:1–15.
41 Asano T, Boisson B, Onodi F, Matuozzo D, Moncada-Velez M, Renkilaraj MRLM, et al. X-linked recessive TLR7 deficiency in ~1% of men under 60 years old with life-threatening COVID-19. Sci Immunol. 2021 Aug;6(62):eabl4348.
42 Zhang Q, Liu Z, Moncada-Velez M, Chen J, Ogishi M, Bigio B, et al. Inborn errors of type I IFN immunity in patients with life-threatening COVID-19. Science (80-). 2020 Oct;370(6515):eabd4570.
43 Akilesh HM, Buechler MB, Duggan JM, Hahn WO, Matta B, Sun X, et al. Chronic TLR7 and TLR9 signaling drives anemia via differentiation of specialized hemophagocytes. Science (80-). 2019;363(6423):eaao5213.

44 Kawai T, Sato S, Ishii KJ, Coban C, Hemmi H, Yamamoto M, et al. Interferon-alpha induction through Toll-like receptors involves a direct interaction of IRF7 with MyD88 and TRAF6. Nat Immunol. 2004 Oct;5(10):1061–8.
45 Ito T, Amakawa R, Kaisho T, Hemmi H, Tajima K, Uehira K, et al. Brief Definitive Report Interferon-and Interleukin-12 Are Induced Differentially by Toll-like Receptor 7 Ligands in Human Blood Dendritic Cell Subsets. 2002;195(11):1507–12.
46 Nahid MA, Benso LM, Shin JD, Mehmet H, Hicks A, Ramadas RA. TLR4, TLR7/8 agonist-induced miR-146a promotes macrophage tolerance to MyD88-dependent TLR agonists. J Leukoc Biol. 2016 Aug;100(2):339–49.
47 Odoardi N, Kourko O, Petes C, Basta S, Gee K. TLR7 Ligation Inhibits TLR8 Responsiveness in IL-27-Primed Human THP-1 Monocytes and Macrophages. J Innate Immun. 2021;13(6):345–58.
48 Michaelis KA, Norgard MA, Levasseur PR, Olson B, Burfeind KG, Buenafe AC, et al. Persistent Toll-like receptor 7 stimulation induces behavioral and molecular innate immune tolerance. Brain Behav Immun. 2019;82(May):338–53.
49 Salagianni M, Galani IE, Lundberg AM, Davos CH, Varela A, Gavriil A, et al. Toll-like receptor 7 protects from atherosclerosis by constraining “inflammatory” macrophage activation. Circulation. 2012 Aug;126(8):952–62.
50 Karadimou G, Plunde O, Pawelzik SC, Carracedo M, Eriksson P, Franco-Cereceda A, et al. TLR7 Expression Is Associated with M2 Macrophage Subset in Calcific Aortic Valve Stenosis. Cells. 2020 Jul;9(7):1710.
51 Riera-Borrull M, Cuevas VD, Alonso B, Vega MA, Joven J, Izquierdo E, et al. Palmitate Conditions Macrophages for Enhanced Responses toward Inflammatory Stimuli via JNK Activation. J Immunol. 2017;199(11):3858–69.
52 Chen EY, Tan CM, Kou Y, Duan Q, Wang Z, Meirelles G V., et al. Enrichr: Interactive and collaborative HTML5 gene list enrichment analysis tool. BMC Bioinformatics. 2013;14:128.
53 Kuleshov M V, Jones MR, Rouillard AD, Fernandez NF, Duan Q, Wang Z, et al. Enrichr: a comprehensive gene set enrichment analysis web server 2016 update. Nucleic Acids Res. 2016;44(W1):W90–7.
54 Subramanian A, Tamayo P, Mootha VK, Mukherjee S, Ebert BL, Gillette MA, et al. Gene set enrichment analysis: a knowledge-based approach for interpreting genome-wide expression profiles. Proc Natl Acad Sci U S A. 2005;102(43):15545–50.
55 Curtis C, Shah SP, Chin SF, Turashvili G, Rueda OM, Dunning MJ, et al. The genomic and transcriptomic architecture of 2,000 breast tumours reveals novel subgroups. Nature. 2012;486(7403):346–52.
56 Pereira B, Chin SF, Rueda OM, Vollan HKM, Provenzano E, Bardwell HA, et al. The somatic mutation profiles of 2,433 breast cancers refines their genomic and transcriptomic landscapes. Nat Commun. 2016;7:11479.
57 Nuzzi PA, Lokuta MA, Huttenlocher A. Analysis of Neutrophil Chemotaxis. Methods Mol Biol. 2007;370:23–35.
58 Vento-Tormo R, Efremova M, Botting RA, Turco MY, Vento-Tormo M, Meyer KB, et al. Single-cell reconstruction of the early maternal–fetal interface in humans. Nature. 2018;563(7731):347–53.
59 Puig-Kröger A, Sierra-Filardi E, Domínguez-Soto A, Samaniego R, Corcuera MT, Gómez-Aguado F, et al. Folate receptor β is expressed by tumor-associated macrophages and constitutes a marker for M2 anti-inflammatory/regulatory Macrophages. Cancer Res. 2009;69(24):9395–403.
60 Cresswell GM, Wang B, Kischuk EM, Broman MM, Alfar RA, Vickman RE, et al. Folate Receptor Beta Designates Immunosuppressive Tumor-Associated Myeloid Cells That Can Be Reprogrammed with Folate-Targeted Drugs. Cancer Res. 2021 Feb;81(3):671–84.
61 Cassetta L, Fragkogianni S, Sims AH, Swierczak A, Forrester LM, Zhang H, et al. Human Tumor-Associated Macrophage and Monocyte Transcriptional Landscapes Reveal Cancer-Specific Reprogramming, Biomarkers, and Therapeutic Targets. Cancer Cell. 2019;35(4):588-602.e10.
62 Zhang F, Ayaub EA, Wang B, Puchulu-Campanella E, Li Y, Hettiarachchi SU, et al. Reprogramming of profibrotic macrophages for treatment of bleomycin-induced pulmonary fibrosis. EMBO Mol Med. 2020 Aug;12(8):e12034.
63 Strieter RM, Gomperts BN, Keane MP. The role of CXC chemokines in pulmonary fibrosis. J Clin Invest. 2007;117(3):549–56.
64 Vlach J, Bender AT, Przetak M, Pereira A, Deshpande A, Johnson TL, et al. Discovery of M5049: A Novel Selective Toll-Like Receptor 7/8 Inhibitor for Treatment of Autoimmunity. J Pharmacol Exp Ther. 2021 Mar;376(3):397–409.
65 Kim H. The transcription factor MafB promotes anti-inflammatory M2 polarization and cholesterol efflux in macrophages. Sci Rep. 2017;7(1):7591.

66 Liu M, Tong Z, Ding C, Luo F, Wu S, Wu C, et al. Transcription factor c-Maf is a checkpoint that programs macrophages in lung cancer. J Clin Invest. 2020;130(4):2081–96.
67 Goudot C, Coillard A, Villani AC, Gueguen P, Cros A, Sarkizova S, et al. Aryl Hydrocarbon Receptor Controls Monocyte Differentiation into Dendritic Cells versus Macrophages. Immunity. 2017;47(3):582-596.e6.
68 Kimura A, Naka T, Nakahama T, Chinen I, Masuda K, Nohara K, et al. Aryl hydrocarbon receptor in combination with Stat1 regulates LPS-induced inflammatory responses. J Exp Med. 2009;206(9):2027–35.
69 Asselin-Paturel C, Trinchieri G. Production of type I interferons: Plasmacytoid dendritic cells and beyond. J Exp Med. 2005;202(4):461–5.
70 Funk E, Kottilil S, Gilliam B, Talwani R. Tickling the TLR7 to cure viral hepatitis. J Transl Med. 2014;12(1):129.
71 Bourgeois C, Majer O, Frohner IE, Lesiak-Markowicz I, Hildering K-S, Glaser W, et al. Conventional Dendritic Cells Mount a Type I IFN Response against Candida spp. Requiring Novel Phagosomal TLR7-Mediated IFN-β Signaling . J Immunol. 2011;186(5):3104–12.
72 Wang H, Yuan M, Wang S, Zhang L, Zhang R, Zou X, et al. STAT3 Regulates the Type I IFN-mediated antiviral response by interfering with the nuclear entry of STAT1. Int J Mol Sci. 2019;20(19):4870.
73 Matsuyama T, Kubli SP, Yoshinaga SK, Pfeffer K, Mak TW. An aberrant STAT pathway is central to COVID-19. Cell Death Differ. 2020;27(12):3209–25.
74 Tsai MH, Pai LM, Lee CK. Fine-tuning of type I interferon response by STAT3. Front Immunol. 2019;10(JUN):1448.
75 Nathan C. Neutrophils and COVID-19: Nots, NETs, and knots. J Exp Med. 2020;217(9):e20201439.
76 Reusch N, De Domenico E, Bonaguro L, Schulte-Schrepping J, Baßler K, Schultze JL, et al. Neutrophils in COVID-19. Front Immunol. 2021;12:652470.
77 Zeng ZY, Feng SD, Chen GP, Wu JN. Predictive value of the neutrophil to lymphocyte ratio for disease deterioration and serious adverse outcomes in patients with COVID-19: a prospective cohort study. BMC Infect Dis. 2021;21(1):80.
78 Park JH, Lee HK. Re-analysis of Single Cell Transcriptome Reveals That the NR3C1-CXCL8-Neutrophil Axis Determines the Severity of COVID-19. Front Immunol. 2020;11:2145.
79 Koenig LM, Boehmer DFR, Metzger P, Schnurr M, Endres S, Rothenfusser S. Blocking inflammation on the way: Rationale for CXCR2 antagonists for the treatment of COVID-19. J Exp Med. 2020;217(9):e20201342.
80 Saeed S, Quintin J, Kerstens HH, Rao NA, Aghajanirefah A, Matarese F, et al. Epigenetic programming of monocyte-to-macrophage differentiation and trained innate immunity. Science (80-). 2014;345(6204):1251086.
81 Feldman C, Anderson R. The role of co-infections and secondary infections in patients with COVID-19. Pneumonia. 2021;13(1):5.
82 Stefan N, Birkenfeld AL, Schulze MB. Global pandemics interconnected — obesity, impaired metabolic health and COVID-19. Nat Rev Endocrinol. 2021;17(3):135–49.
83 Joshi C, Jadeja V, Zhou H. Molecular mechanisms of palmitic acid augmentation in covid-19 pathologies. Int J Mol Sci. 2021;22(13):7127.
84 Boden G. Obesity, insulin resistance and free fatty acids. Curr Opin Endocrinol Diabetes Obes. 2011;18(2):139–43.
85 Sobczak AIS, Blindauer CA, Stewart AJ. Changes in plasma free fatty acids associated with type-2 diabetes. Nutrients. 2019;11(9):2022.
86 González-Domínguez É, Domínguez-Soto Á, Nieto C, Flores-Sevilla JL, Pacheco-Blanco M, Campos-Peña V, et al. Atypical Activin A and IL-10 Production Impairs Human CD16+ Monocyte Differentiation into Anti-Inflammatory Macrophages. J Immunol. 2016;196(3):1327–37.

FIGURE LEGENDS

Figure 1.- Regulated expression of TLR7 in human macrophages. **A**. Schematic representation of the *in vitro* generation of M-MØ and GM-MØ from peripheral blood monocytes. *TLR7* gene expression (normalized fluorescence intensity) in M-MØ and GM-MØ, as determined in microarray experiments (GSE68061) on three independent samples. Statistically significant differences (adjp) are indicated. **B**. TLR7 protein levels in four independent preparations of M-MØ and GM-MØ, as determined by Western blot (Left panel). Relative level of TLR7, including both the full-length (140 kDa) and the proteolytically processed mature (75 kDa) forms, were determined in M-MØ and GM-MØ by densitometry. Mean ± SEM of four independent samples is shown (***, p<0.001). **C**. Relative *TLR7* gene expression in Monocytes, M-MØ and GM-MØ, as determined by RNA-sequencing (GSE188278) on three independent samples. Statistically significant differences are indicated. **D**. *TLR7* gene expression in M-MØ before and after exposure to GM-CSF (1000U/ml) for 24 or 48 hours, and either with or without medium replacement, as determined by RT-PCR. Mean and SEM of four independent experiments are shown (**, p<0.005). **E**. TLR7 gene expression in M-MØ generated from control individuals (2 independent donors) or an MCTO patient (two distinct samples derived from a single MCTO patient), as determined by RNA-sequencing (GSE155883). Statistically significant differences are indicated. **F**. *TLR7* gene expression in M-MØ and GM-MØ before and after LPS activation, as determined in microarray experiments (GSE99056) on three independent samples. Statistically significant differences (adjp) are indicated. **G**. t-Distributed stochastic neighbor embedding plots (t-SNE, Perplexity:25, Colour plot by k=10) illustrating *TLR7*, *MAFB* and *FOLR2* gene expression in the human fetal-maternal interface [58] (https://www.ebi.ac.uk/gxa/sc/home). The "Expression level" bar indicates the expression level in each case (Smartseq 2 data; CPM, counts per million).

Figure 2.- Analysis of the M-MØ response to CL264: Intracellular signaling, cytokine profile and gene signature. **A.** Schematic representation of the treatment of M-MØ for analysis of the intracellular signaling initiated by either LPS or CL264. **B**. Levels of phosphorylated ERK (*p*-ERK), Phosphorylated JNK (*p*-JNK), phosphorylated p38MAPK (*p*-p38) and I□B□ in untreated (-), LPS-treated (LPS, 10ng/ml) and CL264-treated (CL264, 1□g/ml) after 15min, 30min or 45min of stimulation, as determined by Western blot. In each case, 2-5 independent macrophage samples were analyzed, and a representative experiment is shown. Protein loading was normalized after determination of the level of vinculin in each case. **C**. Levels of phosphorylated STAT1 (*p*-STAT1), Phosphorylated STAT3 (*p*-STAT3) and phosphorylated CREB (*p*-CREB) in untreated (-), LPS-treated (LPS, 10ng/ml) and CL264-treated (CL264, 1□g/ml) at the indicated time points, as determined by Western blot. In each case, three independent donors were performed, and a representative donor is shown. Protein loading was normalized after determination of the level of GAPDH in each case. **D**. Schematic representation of the treatment of M-MØ for determination of cytokines released from after exposure to either LPS or CL264. **E**. Production of the indicated cytokines/chemokines in M-MØ untreated (-) or treated for 15hr with either LPS (10ng/ml) or three different concentrations of CL264 (0.1, 1 and 10□g/ml), as determined by ELISA. Mean ± SEM of 3-5 independent donors are shown (Relative to untreated M-MØ: *, p<0.05; **, p<0.01. Relative to LPS-treated M-MØ: #, p<0.05). **F**. Schematic representation of the treatment of M-MØ with either LPS (10ng/ml), CL264 (1□g/ml) or untreated before RNAseq (GSE156921). **G**. *IFNB1* expression in untreated M-MØ, LPS-treated M-MØ and CL264-treated M-MØ at different time points after stimulation, as determined by RNA-seq (GSE156921). **H**. Heatmap of the relative expression of the genes within the "Reactome_2016_genes" (Enrichr) in LPS-treated and CL264-treated M-MØ at the indicated time points after stimulation [log2FC(LPSvsCNT) - log2FC(CL264vsCNT)], as determined by RNAseq (GSE156921) and using Genesis (https://genome.tugraz.at/genesisclient/genesisclient_description.shtml).

Figure 3.- TLR7 conditions the M-MØ responses to later stimuli. **A.** Schematic representation of the treatment of M-MØ with CL264 (1□g/ml) for analysis of changes in the gene expression profile. **B**. Relative expression of the indicated genes of the M-MØ-specific "Anti-inflammatory gene set" (blue) and GM-MØ-specific "Pro-inflammatory gene set" (red) in untreated (-) and CL264-treated M-MØ, as determined by quantitative RT-PCR on six macrophage samples derived from six independent donors. Mean ± SEM are shown (*, p<0.05). **C.** GSEA of the GM-MØ-specific "Pro-inflammatory gene set" (left panel) or M-MØ-specific "Anti-inflammatory gene set" (right panel) on the ranked comparison of CL264-treated M-MØ and untreated M-MØ at 12 hr after stimulation (GSE156921). Normalized Enrichment Score (NES) and FDRq values are indicated. **D**. Schematic representation of the sequential treatment of CL264-treated with CL264 (1□g/ml) or LPS (10ng/ml) for analysis of intracellular signaling (30 or 60 min) and cytokine

production (after 16h). **E.** Levels of phosphorylated ERK (p-ERK), Phosphorylated JNK (p-JNK), phosphorylated STAT3 (p-STAT3), phosphorylated STAT1 (p-STAT1) and I□B□ in M-MØ exposed to the indicated primary and secondary stimuli after 30min (p-ERK, p-JNK, IkB□) or 60min (p-STAT1, p-STAT3) of stimulation, as determined by Western blot. In each case, four macrophage samples derived from four independent donors were analyzed, and a representative experiment is shown. Protein loading was normalized after determination of the level of vinculin in each case. **F**. Production of the indicated cytokines in M-MØ was evaluated after exposure to the indicated primary (24 hours) and secondary (16 hours) stimuli, as determined by ELISA. Mean ± SEM of four independent donors are shown (*, p<0.05; **, p<0.01).

Figure 4.- TLR7 activation of M-MØ induces neutrophil-attracting chemokines. **A.** k-means clustering of the 467 genes differentially expressed (|log2FC|>3) at any time point between LPS-treated M-MØ and CL264-treated M-MØ (GSE156921). For each gene, expression level in the three donors are represented after normalizing gene expression and k-means clustering using Genesis (http://genome.tugraz.at/genesisclient/). The identity of some genes within each cluster is indicated. **B**. Heatmap of the expression of the indicated chemokine-encoding genes in LPS-treated M-MØ and CL264-treated M-MØ at the indicated time points after stimulation (GSE156921). **C**. GSEA of the "GOBP_NEUTROPHIL_CHEMOTAXIS" gene set on the ranked comparison of the transcriptomes of CL264-treated M-MØ and untreated M-MØ at 12hr after stimulation (GSE156921). Normalized Enrichment Score (NES) and FDRq values are indicated. **D**. Production of the indicated chemokines in untreated (-) M-MØ, LPS-treated (10ng/ml) and CL264-treated (1□g/ml) M-MØ (16h), as determined by ELISA. Mean ± SEM of four independent donors are shown (*, p<0.05). **E**. Neutrophil migration in response to IL-8 or culture supernatants from untreated M-MØ or CL264-treated (1□g/ml) M-MØ, as determined by Transwell migration assays. Mean ± SEM of four independent donors are shown (**, p<0.01). **F**. Production of the indicated cytokines in M-MØ was evaluated after exposure to the indicated primary stimulus (24 hours) and secondary stimulus (16 hours), as determined by ELISA. Mean ± SEM of four independent donors are shown (**, p<0.01).

Figure 5.- The acquisition of the TLR7-specific transcriptome and neutrophil-recruiting chemokine production depends on the macrophage polarization state. **A.** Schematic representation of siRNA-mediated gene silencing before treatment of M-MØ with CL264 (1□g/ml) for determination of the gene expression profile. **B**. Summary of GSEA of the Clusters identified in Figure 4 on the ranked comparison of the transcriptomes of CL264-treated (4h) siAHR M-MØ [siAHR M-MØ+CL264 (*left panel*)], siMAF M-MØ [siMAF M-MØ+CL264 (*middle panel*)] or siMAFB M-MØ [siMAFB M-MØ+CL264 (*right panel*)] versus siCNT M-MØ+CL264. FDRq value is indicated in each case. **C**. Relative expression of the indicated chemokine-encoding genes in CL264-treated (4h) siAHR M-MØ, siMAF M-MØ and siMAFB M-MØ [log2FC (siTF-MMØ+CL264 / siCNT-MMØ+CL264)], as determined by RNA-Seq (*, adjp<0.05). **D**. Schematic representation of siRNA-mediated gene silencing before treatment of M-MØ with CL264 (1□g/ml) for determination of the cytokine profile. **E**. Production of the indicated chemokines in untreated M-MØ (-), siCNT M-MØ+CL264, siAHR M-MØ+CL264, siMAF M-MØ+CL264 and siMAFB M-MØ+CL264, as determined by ELISA. Data represent the production of chemokines by each cell type relative to the levels produced by siCNT M-MØ+CL264. Mean ± SEM of three independent donors are shown (*, p<0.05; **, p<0.01).

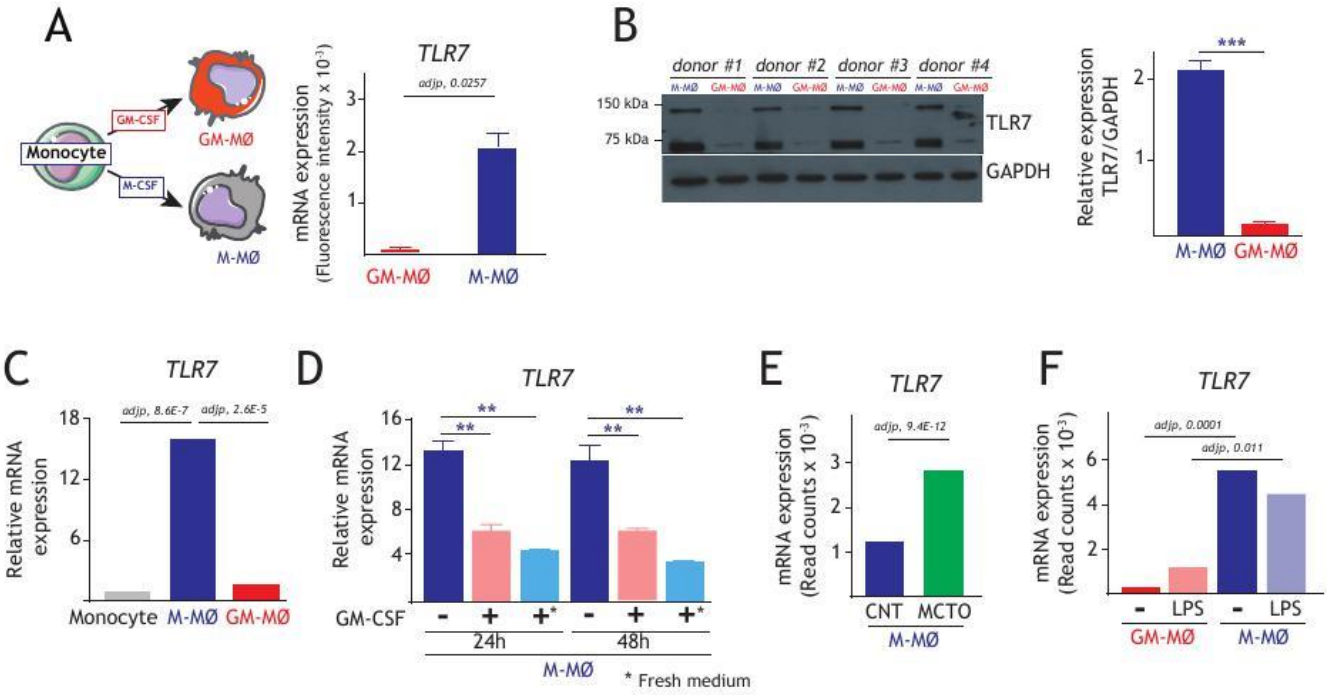
A
Monocyte
GM-CSF
M-CSF
GM-MØ
M-MØ
TLR7
adjp, 0.0257
mRNA expression (Fluorescence intensity x 10-3)
GM-MØ
M-MØ
B
donor #1
donor #2
donor #3
donor #4
M-MØ
GM-MØ
150 kDa
75 kDa
TLR7
GAPDH
Relative expression TLR7/GAPDH
***
M-MØ
GM-MØ
C
TLR7
adjp, 8.6E-7
adjp, 2.6E-5
Relative mRNA expression
Monocyte
M-MØ
GM-MØ
D
TLR7
Relative mRNA expression
GM-CSF
24h
48h
M-MØ
* Fresh medium
E
TLR7
adjp, 9.4E-12
mRNA expression (Read counts x 10-3)
CNT
MCTO
M-MØ
F
TLR7
adjp, 0.0001
adjp, 0.011
mRNA expression (Read counts x 10-3)
LPS
GM-MØ
M-MØ
G
Clusters
TLR7
MAFB
FOLR2
Monocytes
NK cells
T cells
Macrophages
Stromal cells

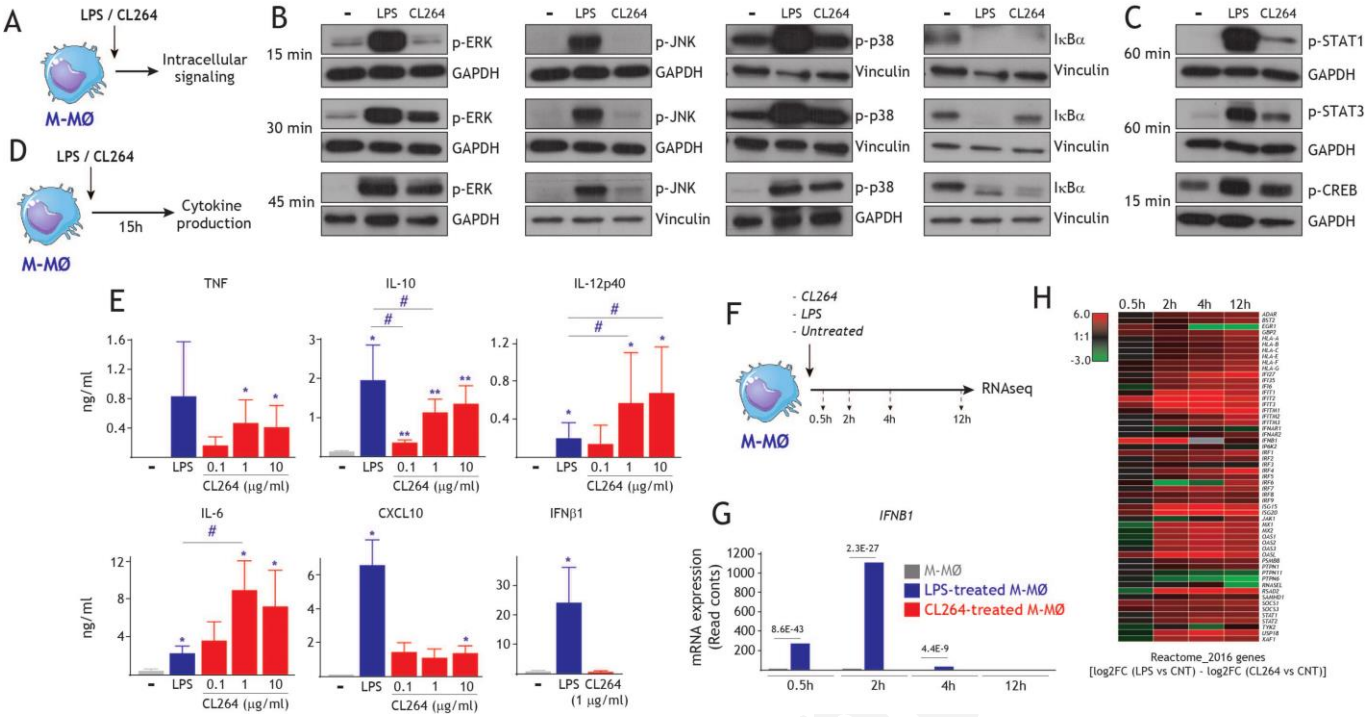

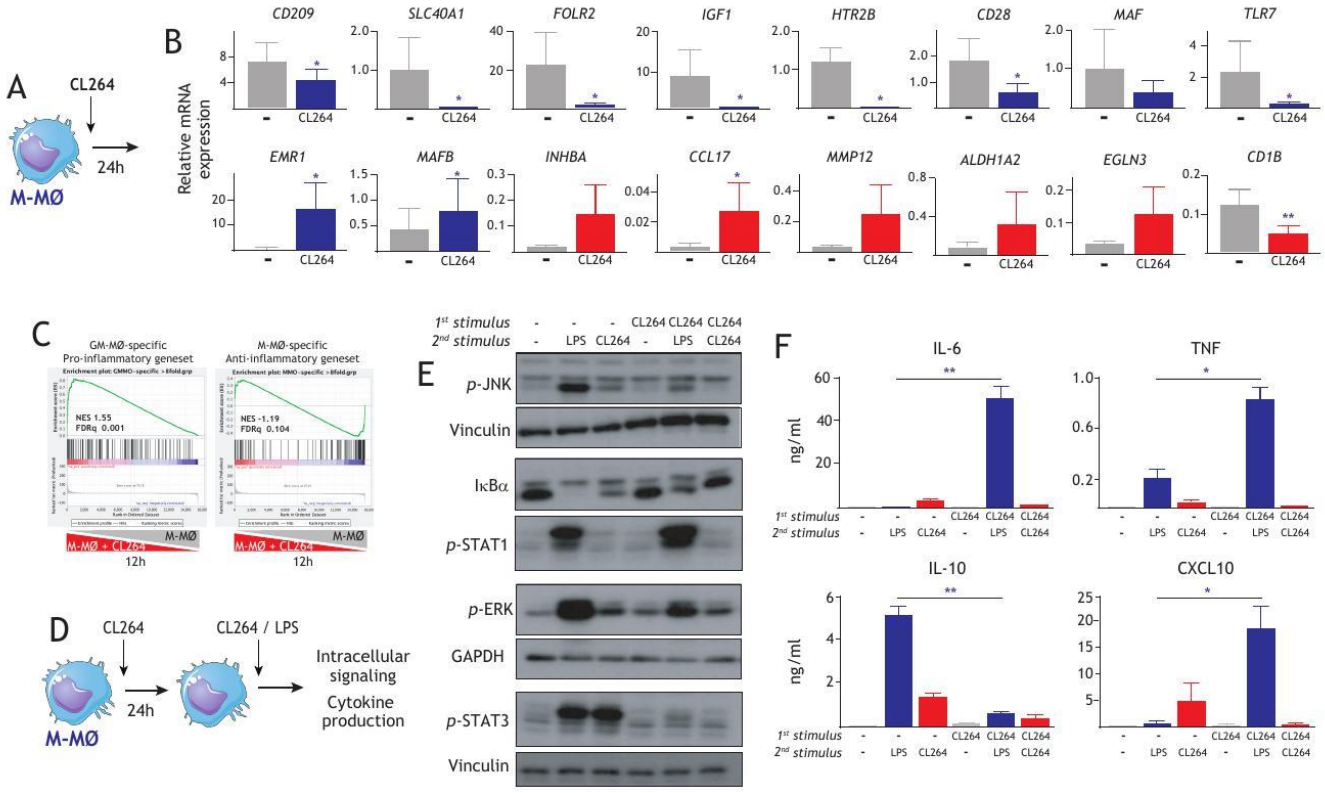
A
CL264
24h
M-MØ
B
Relative mRNA expression
CD209
SLC40A1
FOLR2
IGF1
HTR2B
CD28
MAF
TLR7
EMR1
MAFB
INHBA
CCL17
MMP12
ALDH1A2
EGLN3
CD1B
-
CL264
C
GM-MØ-specific
Pro-inflammatory geneset
M-MØ-specific
Anti-inflammatory geneset
NES 1.55
FDRq 0.001
NES -1.19
FDRq 0.104
M-MØ
M-MØ + CL264
12h
D
CL264
CL264 / LPS
24h
M-MØ
Intracellular signaling
Cytokine production
E
1st stimulus
2nd stimulus
p-JNK
Vinculin
IκBα
p-STAT1
p-ERK
GAPDH
p-STAT3
Vinculin
F
IL-6
TNF
IL-10
CXCL10
ng/ml

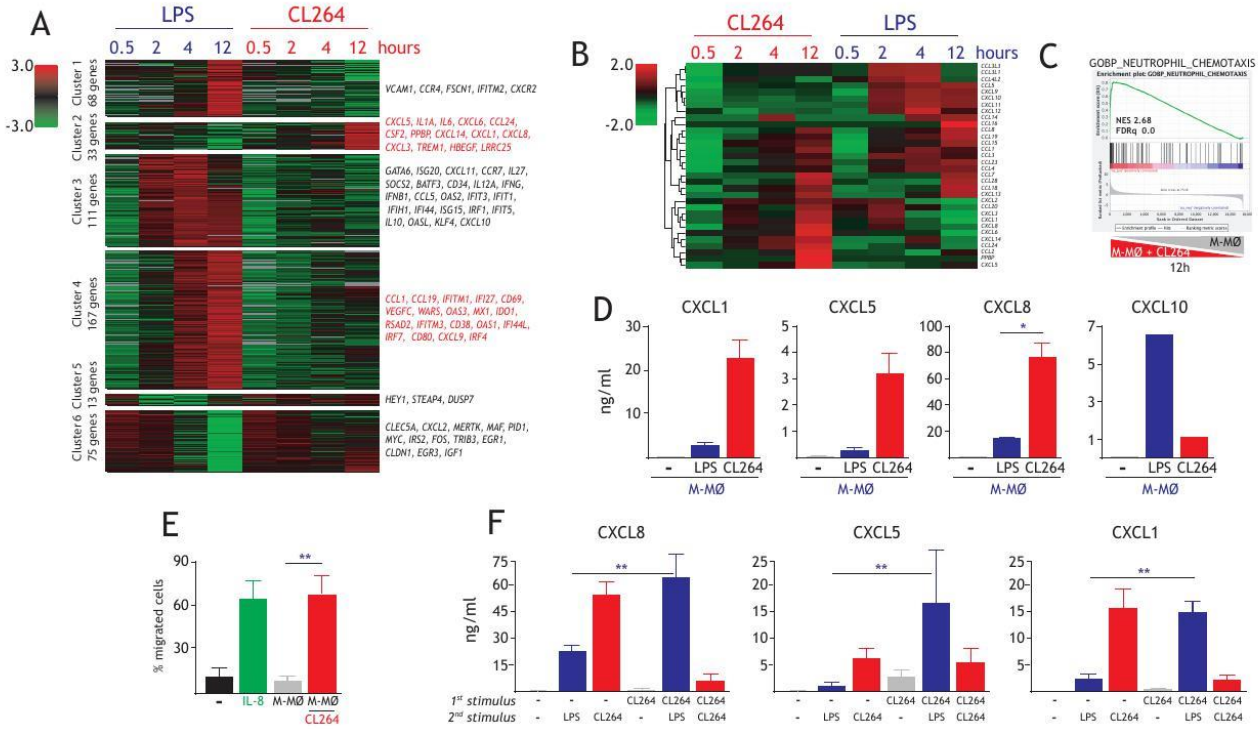
A
LPS
CL264
0.5 2 4 12 0.5 2 4 12 hours
3.0
-3.0
Cluster 1 68 genes
VCAM1, CCR4, FSCN1, IFITM2, CXCR2
Cluster 2 33 genes
CXCL5, IL1A, IL6, CXCL6, CCL24, CSF2, PPBP, CXCL14, CXCL1, CXCL8, CXCL3, TREM1, HBEGF, LRRC25
Cluster 3 111 genes
GATA6, ISG20, CXCL11, CCR7, IL27, SOCS2, BATF3, CD34, IL12A, IFNG, IFNB1, CCL5, OAS2, IFIT3, IFIT1, IFIH1, IFI44, ISG15, IRF1, IFIT5, IL10, OASL, KLF4, CXCL10
Cluster 4 167 genes
CCL1, CCL19, IFITM1, IFI27, CD69, VEGFC, WARS, OAS3, MX1, IDO1, RSAD2, IFITM3, CD38, OAS1, IFI44L, IRF7, CD80, CXCL9, IRF4
Cluster 5 13 genes
HEY1, STEAP4, DUSP7
Cluster 6 75 genes
CLEC5A, CXCL2, MERTK, MAF, PID1, MYC, IRS2, FOS, TRIB3, EGR1, CLDN1, EGR3, IGF1
B
CL264
LPS
0.5 2 4 12 0.5 2 4 12 hours
2.0
-2.0
C
GOBP_NEUTROPHIL_CHEMOTAXIS
NES 2.68
FDRq 0.0
M-MØ
M-MØ + CL264
12h
D
CXCL1
CXCL5
CXCL8
CXCL10
ng/ml
- LPS CL264
M-MØ
E
% migrated cells
- IL-8 M-MØ M-MØ CL264
F
CXCL8
CXCL5
CXCL1
ng/ml
1st stimulus
2nd stimulus

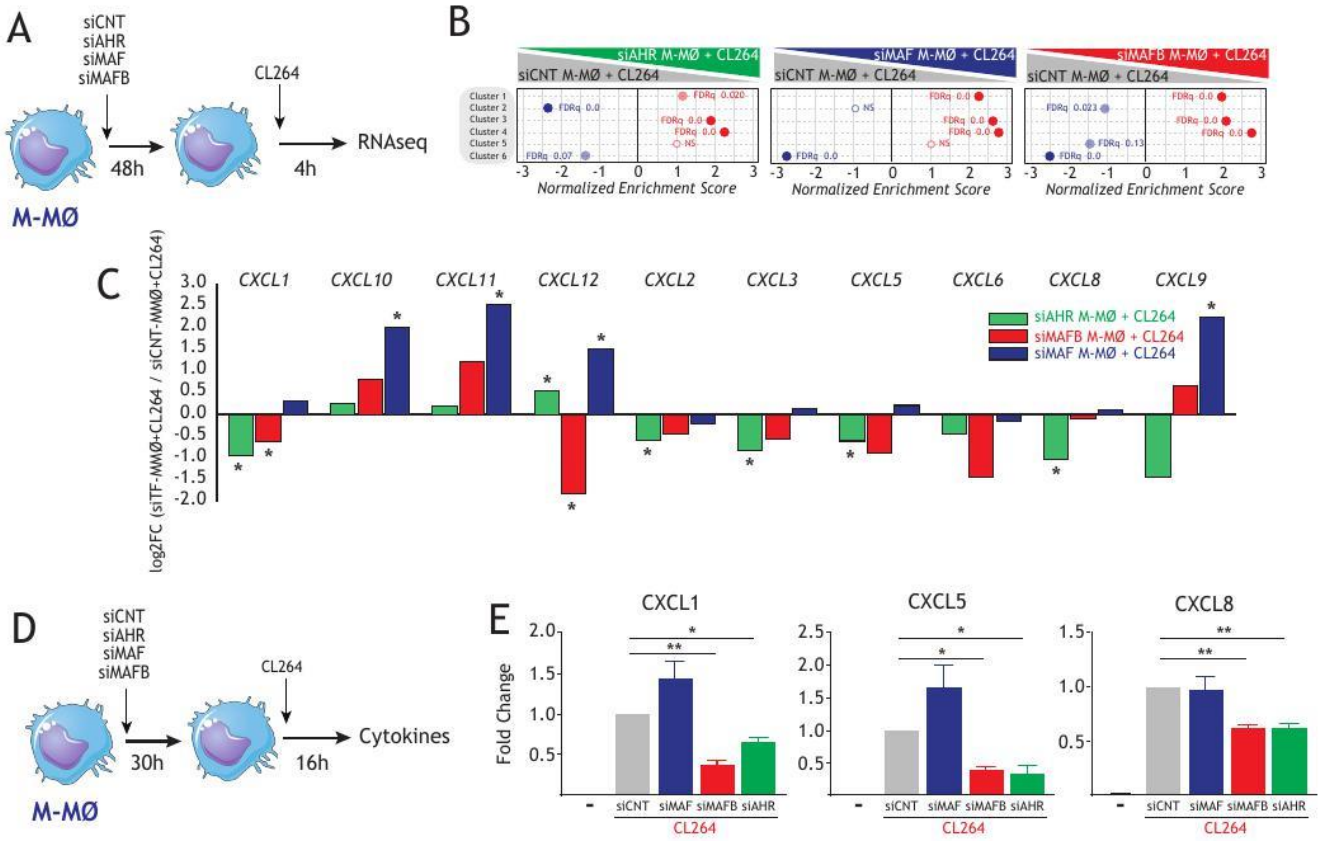
A
siCNT
siAHR
siMAF
siMAFB
48h
CL264
4h
RNAseq
M-MØ
B
siAHR M-MØ + CL264
siCNT M-MØ + CL264
siMAF M-MØ + CL264
siMAFB M-MØ + CL264
Cluster 1
Cluster 2
Cluster 3
Cluster 4
Cluster 5
Cluster 6
Normalized Enrichment Score
C
CXCL1
CXCL10
CXCL11
CXCL12
CXCL2
CXCL3
CXCL5
CXCL6
CXCL8
CXCL9
siAHR M-MØ + CL264
siMAFB M-MØ + CL264
siMAF M-MØ + CL264
log2FC (siTF-MMØ+CL264 / siCNT-MMØ+CL264)
D
siCNT
siAHR
siMAF
siMAFB
30h
CL264
16h
Cytokines
M-MØ
E
CXCL1
CXCL5
CXCL8
Fold Change
siCNT
siMAF
siMAFB
siAHR
CL264